# Deciphering the Dynamic Molecular Program of Radiation-Induced Endothelial Senescence

Mohamed Amine Benadjaoud, Frédéric Soysouvanh, Georges Tarlet, Vincent Paget, Valerie Buard, Henrique Santos de Andrade, Ian Morilla, Morgane dos Santos, Annaig Bertho, Bruno L'Homme, et al.

INTERNATIONAL JOURNAL OF
RADIATION ONCOLOGY • BIOLOGY • PHYSICS
www.redjournal.org

BIOLOGY CONTRIBUTION

# Deciphering the Dynamic Molecular Program of Radiation-Induced Endothelial Senescence

Mohamed Amine Benadjaoud, PhD,[*,†,2] Frédéric Soysouvanh, PhD,[*,‡,2] Georges Tarlet, BSc,[*] Vincent Paget, PhD,[*] Valérie Buard, BSc,[*] Henrique Santos de Andrade, MSc,[*] Ian Morilla, PhD,[*] Morgane Dos Santos, PhD,[§] Annaïg Bertho, PhD,[*,†] Bruno l'Homme, BSc,[§] Gaëtan Gruel, PhD,[§] Agnès François, PhD,[*] Michele Mondini, PhD,[‖,¶,#,**] Eric Deutsch, MD, PhD,[‖,¶,#,**,††] Olivier Guipaud, PhD,[*] and Fabien Milliat, PhD[*]

[*]*Institute for Radiological Protection and Nuclear Safety (IRSN), Radiobiology of Medical Exposure Laboratory, Fontenay-aux-Roses;* [†]*IRSN, Department of Radiobiology and Regenerative Medicine, Fontenay-aux-Roses;* [‡]*Sorbonne University, Doctoral College, Paris;* [§]*IRSN, Radiobiology of Accidental Exposure Laboratory, Fontenay-aux-Roses;* [‖]*Gustave Roussy, Université Paris-Saclay, SIRIC SOCRATE, Villejuif;* [¶]*French National Institute of Health and Medical Research (INSERM), Villejuif;* [#]*Univ Paris Sud, Université Paris-Saclay, Le Kremlin-Bicêtre;* [**]*INSERM U1030 Gustave Roussy, Villejuif; and* [††]*Gustave Roussy, Université Paris-Saclay, Département de Radiothérapie, Villejuif, France*

Received Sep 22, 2021; Accepted for publication Nov 15, 2021

**Purpose:** Radiation-induced cellular senescence is a double-edged sword, acting as both a tumor suppression process limiting tumor proliferation, and a crucial process contributing to normal tissue injury. Endothelial cells play a role in normal tissue injury after radiation therapy. Recently, a study observed an accumulation of senescent endothelial cells (ECs) around radiation-induced lung focal lesions following stereotactic radiation injury in mice. However, the effect of radiation on EC senescence remains unclear because it depends on dose and fractionation, and because the senescent phenotype is heterogeneous and dynamic.

**Methods and Materials:** Using a systems biology approach in vitro, we deciphered the dynamic senescence-associated transcriptional program induced by irradiation.

**Results:** Flow cytometry and single-cell RNA sequencing experiments revealed the heterogeneous senescent status of irradiated ECs and allowed to deciphered the molecular program involved in this status. We identified the Interleukin-1 signaling pathway as a key player in the radiation-induced premature senescence of ECs, as well as the endothelial-to-mesenchymal transition process, which shares strong hallmarks of senescence.

**Conclusions:** Our work provides crucial information on the dynamics of the radiation-induced premature senescence process, the effect of the radiation dose, as well as the molecular program involved in the heterogeneous senescent status of ECs. 

Corresponding author: E-mail: fabien.milliat@irsn.fr

This work was supported by the IRSN (Institute for Radiological Protection and Nuclear Safety—ROSIRIS program), the Canceropôle d'Ile de France INCa Institut National du Cancer (INCa 2018-1-PLBIO-06), and Electricité de France (EDF-GGP Radioprotection). This work is part of the collaborative program between IRSN and Gustave Roussy (2021-2025): Integrated Preclinical Research Project on the Radiobiology of Tumors and Healthy Tissues (PIRATT).

Disclosures: none.

The data that support the findings of this study are available from the corresponding author upon reasonable request.

Supplementary material associated with this article can be found, in the online version, at doi:10.1016/j.ijrobp.2021.11.019.

*Acknowledgements*—We thank the Groupe de Soutien à l'Experimentation Animale (Animal Experiment Support Group) at IRSN for their excellent technical assistance.

[2] Mohamed Amine Benadjaoud and Frédéric Soysouvanh are co-first authors of this study.



https://doi.org/10.1016/j.ijrobp.2021.11.019

## Introduction

Senescence is characterized by a durable cell cycle arrest and a persistent pro-inflammatory phenotype known as the senescence-associated secretory phenotype.[1,2] Senescence occurs during the aging process but also occurs prematurely in response to stress, as a variable process depending on both the cell type and the stressor.[3,4] Radiation can induce premature senescence, and interest in research into the role of senescence in the benefit-risk ratio after radiotherapy is growing.[5] Radiation-induced cellular senescence is a double-edged sword, acting as both a tumor suppression process limiting tumor proliferation and a crucial process contributing to normal tissue injury.

Ionizing radiation promotes senescence in most cell types, including endothelial cells (ECs).[6-9] Using $p16^{INK4}$-LUC knock-in mice, a study recently reported that lung stereotactic body radiation therapy leads to senescence.[10] Stereotactic body radiation therapy induces acute and very long-term $p16^{INK4}$ activation in the irradiated lung target volume associated with fibrosis and a panel of heterogeneous senescent cells including pneumocytes, macrophages, and ECs, suggesting that these senescent cell types could contribute to radiation injury. Moreover, a study on hemithorax irradiation in mice treated with ABT-263, a Bcl-2 inhibitor, provided the proof of concept that senolytic drugs could be a good strategy for limiting radiation-induced normal tissue injury, more precisely for reducing the level of senescent type II pneumocytes.[11]

The role of the endothelium in radiation-induced normal tissue injury has been debated for many years, mainly surrounding the existence—or not—of endothelial apoptosis.[12-14] Using VE-CADcre or $creER^{T2}$ transgenic mice models allowing specific endothelial genetic deletion, it was demonstrated that ECs contribute significantly to radiation-induced normal tissue injury and to the associated wound healing process.[15-17] Thus, mice with endothelial deletion of plasminogen activator inhibitor-1 (also known as SERPINE1), a strong mediator of cell senescence, are protected from normal tissue injury.[12,16,18,19] However, the effect of radiation on EC senescence remains unclear because it depends on several parameters, such as the organ exposed, fractionation, dose, and temporality of the observation. Because the senescent phenotype is heterogeneous,[20] dynamic,[21] and specific to cell types, the identification of EC dynamic signatures to understand the senescence program is crucial in developing specific therapeutic strategies for senescence-associated vascular dysfunction. In this interdisciplinary work, we investigated in depth how ionizing radiation modifies the kinetics of the senescence transcription program in ECs.

## Methods and Materials

### Cell culture and irradiation procedure

We sourced primary human umbilical vein EC (HUVEC, pooled donor), human lung microvascular EC, human dermal microvascular EC, human heart microvascular EC, and human pulmonary artery EC from Lonza (Verviers, Belgium). We isolated human intestinal microvascular EC from surgically resected specimens of normal human colon, as previously described.[22] We cultured all cells in EGM-2MV medium (Lonza) supplemented by 12 mg/mL Bovine Brain Extract without heparin for HMVEC-L (Lonza).

Confluent cells were x-ray irradiated using a medical linear accelerator (Elekta Synergy Platform, Elekta SAS, Boulogne-Billancourt, France; 4 MV; dose rate 2.5 $Gy.min^{-1}$ in air kerma free in air). The medium was changed before irradiation and every 7 days thereafter.

### Senescence ($C_{12}$FDG)/Generation (CellTrace) by flow cytometry

Before irradiation, confluent monolayers of HUVECs were washed twice with PBS 1X (with $Ca^{2+}$ and $Mg^{2+}$), then stained for 20 min with 7.5 $\mu$M final of CellTrace Violet (Thermo Fisher Scientific). Cells were then irradiated to 2, 4, 5, 6, 10, or 20 Gy + control (nonirradiated). Seven days after irradiation, senescence experiments were performed following the Debacq-Chainiaux et al protocol[23] and detailed in Appendix E1.

### Single-cell RNA-Seq experiments

HUVECs were trypsinized and stained using Trypan blue to ensure viability of 75% to 90%. Approximately $2 \times 10^4$ cells were resuspended for loading on a 10X Chromium Controller (10X Genomics), and scRNA-Seq libraries were prepared using a Single-Cell 3′v3 Reagent Kit according to the manufacturer's protocols. Two independent experiments were performed including 4 experimental conditions: 0 Gy day 0, control cells at the day of the irradiation; 0 Gy day 7; 5 Gy day 7; and 20 Gy day 7 (ie, control and irradiated cells 7 days after irradiation). In total, 8 samples were included in the study. Library quantification and quality assessment was performed using the Agilent Bioanalyzer 2100 (Agilent Genomics). Indexed libraries were equimolarly pooled and sequenced on an Illumina NovaSEq 6000 sequencing system with a minimum depth sequencing at 20,000 read pairs/cell. Single-cell RNA-Seq outputs were processed using the Cell Ranger software (10X Genomics). Analysis were performed using the Seurat and Monocle packages in R as detailed in Appendix E1.

Other experimental procedures are detailed in Appendix E1.

## Results

### Radiation induces a profound senescent phenotype in ECs

To fully decipher the radiation-induced molecular program of ECs, the choice of EC type is crucial. We first compared the response of 6 normal human EC types 7 days after radiation exposure, using a custom TaqMan Low-Density Array to measure the expression levels of 44 mRNAs involved in senescence (see list of genes in Figure E1). Each EC type displays a specific mRNA signature (Fig. E2A), and the transcriptional signature for EC senescence is different for 2 mesenchymal cell types (Fig. E3). For each EC type, we evaluated the concordance between their transcriptional response to irradiation and the first principal component scores of the 5 others. Because the first principal component represents the direction along which the data exhibit the largest variation, this procedure makes it possible to identify the EC type able to summarize the major dispersion of the response of other EC types. Our analysis strongly suggests that HUVECs are the most informative cellular model for the study of endothelial senescence among those tested (Figs. E2B-D). Therefore, we studied radiation-induced senescence in HUVECs and observed typical markers characteristic of stress-induced senescence, ie, cellular hypertrophy, $\beta$-Gal expression in lysosomes, p21 overexpression, and lamin B1 downregulation (Figs. 1A and 1B). Senescence quantification by flow cytometry using $C_{12}$FDG, performed 7 days after 20 Gy exposure, shows a 50% increase in senescent cells (Fig. 1C). We jointly quantified senescence and proliferation using $C_{12}$FDG and CellTrace probes (Figs. 1D and E4). Irradiation-induced dose-dependent $C_{12}$FDG cleavage is associated with an increase in cell size, which plateaued at 6 Gy in correlation with a decrease in proliferation. Moreover, because senescent cells acquire a senescence-associated secretory phenotype (SASP) characterized by the secretion of multiple growth factors and cytokines, we characterized the senescence-messaging secretome (SMS) at 7 and 14 days after exposure to 2, 5, 10, and 20 Gy (Fig. 1E). The secretion of CXCL1/GROa, IGFBP family, IL6, IL8, MMP7, and PAI-1 increased dose dependently (Fig. 1F). Moreover, we explored the ability of the SMS to induce noncell-autonomous effects, that is, paracrine effects. Radiation-induced SMS led nonirradiated HUVECs to acquire strong hallmarks of senescence (Fig. 1G-I).

### Radiation dose−dependent dynamic modification of senescence-associated transcription in EC

We then studied the dynamic molecular transcriptional program associated with senescence after radiation exposure in HUVECs, using 9 irradiation doses and 7 time points (Fig. E5), with a specific dynamic molecular program for each gene according to the radiation dose (Fig. E6). Replicative senescence experiments show that radiation-induced senescence shares a large panel of markers with 9 genes in common between "aging" HUVECs and irradiated HUVECs 21 days after 20 Gy exposure (Fig. E7). We developed mathematical methods suited to dynamic processes to comprehensively analyze the bivariate (dose and time) structure of variance-covariance data and performed dimension reduction prior to a clustering schema by highlighting all main modes of variability. More precisely, a bivariate smoothing process was first performed to smooth the time- and dose-dependent measurements for a bivariate functional object. An example is shown for 5 genes, specifically CDKN1A, TAGLN, SERPINE1, CDK1, and IL8 (Fig. 2A), and the process was performed for all 44 genes (Figs. E8 and E9). Next, a functional principal component analysis was performed to determine the variance structure of the functional data and showed that 4 harmonics explained 90% of the total variability (Fig. 2B). By using this functional data analysis approach, we established day 7 as a transitional time point in our experimental conditions. We then used Lin's concordance correlation coefficient as a similarity measure to establish relevant gene clusters. We identified 4 clusters according to the form of dynamic variation, which can be summarized as "early downregulation," "late upregulation," "downregulation," and "early upregulation" (Fig. 3A). Four genes (IGFBP5, SELP, CSF2, and CAV1) were identified as outliers with respect to the similarity measure (Lin's concordance correlation coefficient) and were not included in the cluster analysis (Fig. E10). Finally, we used text-mining bioinformatics tools to build molecular networks for each cluster (Fig. 3A) and for all data (Fig. 3B). Network inference of the senescence-associated dynamic transcriptional program in our experiments identified the IL-1−dependent signaling pathway as a putative molecular hub, which controls molecular entities from clusters 2, 3, and 4, and from a large panel of SASP-associated secretory proteins.

### Irradiation leads to a heterogeneous senescent status in ECs

An in-depth analysis of the flow cytometry experiments shows the heterogeneous status of senescent cells (Fig. E11). Dynamic analysis indicates that day 7 after irradiation could be a pertinent point at which to observe the transition of the temporal dynamic, so as to explore radiation-induced senescence fate and decipher cell trajectories using computational pseudotime analysis tools (Fig. 2B). To fully characterize the radiation-induced molecular landscape of senescence in HUVECs, we performed single-cell RNA-Seq experiments (Fig. 4A). HUVECs were exposed to 5 Gy or 20 Gy doses and analyzed 7 days after irradiation. Two nonirradiated cell control groups were also included, that is, cells analyzed the day of the irradiation (0 Gy day 0) and cells analyzed 7 days after irradiation (0 Gy day 7, 5 Gy day 7, and 20 Gy

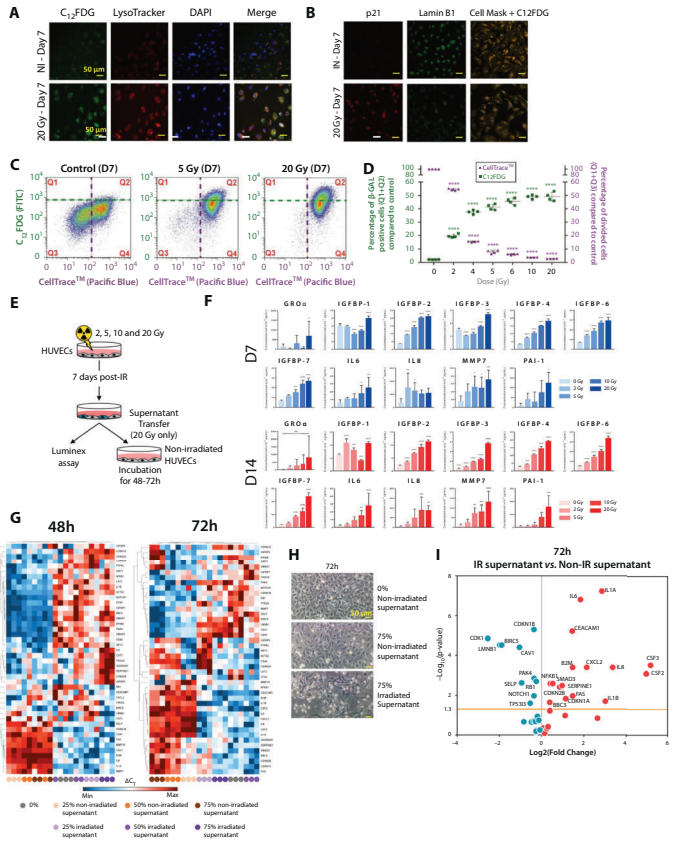


**Fig. 1.** Irradiation induces a senescence-messaging secretome capable of activating a senescence-associated transcriptional program in nonirradiated endothelial cells. (A) Representative images of human umbilical vein endothelial cells (HUVECs) 7 days after 20 Gy. Beta-gal and lysosomes detected using $C_{12}$FDG and Lysotracker counterstained with DAPI. (B) p21 and Lamin B1 representative immunostaining. Beta-gal and hypertrophy detected using $C_{12}$FDG and CellMaskTM. (C) The senescence/proliferation rates were monitored using $C_{12}$FDG cleavage detection and CellTrace Violet by flow cytometry, and representative flow cytometry dot plots were obtained 7 days after 5 or 20 Gy. In control cells, the decrease in CellTrace fluorescence indicates cell division. Irradiated cells incur a stable CellTrace Violet fluorescent signal as well as an increase of $C_{12}$FDG cleavage. (D) Quantification of proliferation and senescence in HUVECs, 7 days after radiation exposure (results are from 4 independent biological replicates). (E) Scheme of experiments: HUVECs were irradiated at 2, 5, 10, and 20 Gy, and cell supernatants were collected 7 or 14 days after irradiation (with a cell medium change at day 7). (F) The dose-dependent secretion of a panel of cytokines was measured by multiplex assays (n=3 biological replicates; mean ± SD are plotted; one-way ANOVA with $^{*}P < .05$, $^{\dagger}P < .01$, $^{\ddagger}P < .001$, and $^{\S}P < .0001$). (G) The gene expression profile of 44 genes involved in the senescence-associated transcriptional program in non-irradiated HUVECs exposed with control conditional medium (7 days' secretion from nonirradiated HUVECs) or a different percentage of cell supernatants collected from HUVECs 7 days after radiation exposure at 20 Gy. The senescence transcriptional program was analyzed at 48 hours and 72 hours after conditional medium incubation in non-irradiated HUVECs. (H) Representative phase microscopy images of nonirradiated HUVECs exposed with control conditional medium or exposed with 75% cell supernatants collected from HUVECs 7 days after radiation exposure at 20 Gy. (I) Volcano plot (72 hours after incubation) showing differentially expressed genes in nonirradiated HUVECs exposed with control conditional medium or exposed with conditional medium from irradiated cells (25%, 50%, and 75% samples are pooled). *Abbreviations:* HUVEC = human umbilical vein endothelial cell; IR = irradiated; non-IR = non-irradiated.

day 7). Two independent experiments were conducted and, after quality control, preprocessing, and batch correction, 56,904 cells were included in the analysis (16,289 cells for 0 Gy day 0; 14,664 cells for 0 Gy day 7; 10,467 cells for 5 Gy day 7; and 15,484 cells for 20 Gy day 7) (Fig. 4B). Although we performed only 2 biological replicates, we obtained an extremely consistent matrix allowing a robust analysis of the effects of irradiation on endothelial cells.These results confirm the heterogeneous status of senescent cells 7 days after irradiation (Figs. 4B-D). We used a panel of 5 key genes involved in senescent status (CDKN1A, TAGLN, SERPINE1, IL8, and CDK1) to understand the data's structuration (Fig. 4C), and the results revealed that, after 20 Gy exposure, all cells expressed high levels of CDKN1A and a

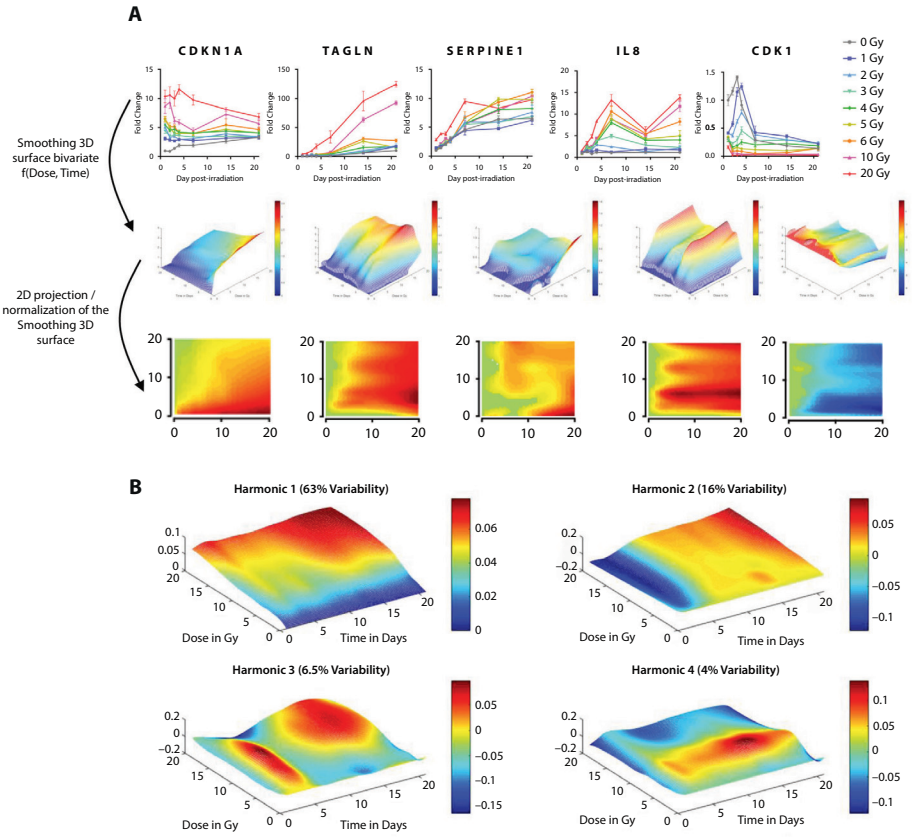


**Fig. 2.** Irradiation dose dependently induces a dynamic senescence-associated transcriptional program in endothelial cells. Human umbilical vein endothelial cells were irradiated at 1, 2, 3, 4, 5, 6, 10, and 20 Gy, and TLDA analyses were performed at different time points, that is, 1, 2, 3, 4, 7, 14, and 21 days post radiation exposure. Results presented are from 2 independent experiments, each performed with 2 biological replicates. (A) For each gene, a classical 2-dimensional to a smoothing 3-dimensional (surface) bivariate f(Dose, Time) process was constructed; examples are shown for CDKN1A (p21), TAGLN, SERPINE1, IL8, and CDK1. All other genes are shown in Figures E8 and E9. For classical representation, results present the fold change (x-axis) with 0 Gy day 1 as a reference at 1 according to time (y-axis) and for each dose. For the 3-dimensional smoothing surface, the results present the fold change (y-axis) with 0 Gy day 1 as a reference at 1 according to time (x-axis) and for each dose (z-axis). The 2-dimensional projection plot of the 3-dimensional smoothing surface presents the dose (x-axis) according to time (y-axis). (B) Plots of the first 4 main functional components (harmonics), describing the variability modes of the 3-dimensional dose-time gene kinetics. These 4 harmonics will be used for the similarity distance-based clustering method. The proportions of explained variance are given between brackets. *Abbreviations:* 2D = 2-dimensional; 3-D = 3-dimensional.

low expression of CDK1. Among the 20 Gy-exposed cells, we identified a subcluster of cells expressing high levels of SERPINE1, CXCL8/IL8, and TAGLN (Fig. 4E). The HMGB2 downregulation and CD9 upregulation previously demonstrated as key molecular entities in replicative senescence were also identified in our work (Figs. E12 and E13).[24,25] To take the study even further, we next used pseudotime analysis and found a node that addresses the cellular fate associated with either a "low senescent" or "high senescent" status in the 20 Gy-exposed cell group (Fig. 4F). A high senescent status is characterized by high levels of SERPINE1, IL8, and TAGLN (cluster 4) (Figs. 4G and 4H). An extensive trajectories analysis revealed the top 10 genes, explaining the global trajectory, mainly composed of genes involved in the cellular proliferation status, such as MKI67, TOP2A, CENPF, and ASPM (Fig. 5A). When we focused our attention on cluster 4 (high senescent status), we identified the von Willebrand factor as the first candidate explaining the trajectory toward a high senescent status (Fig. 5B). The top 300 ranking is given in Table E1. The same analysis strategy was used for the 44 genes of the signature (Fig. E14). When we combined the 44 genes measured in our study and the top 50 genes explaining the trajectory from the RNA-Seq experiments, we could visualize changes for those genes through pseudotime as well as modules of genes that have similar expression patterns (Fig. 5C). These results revealed that a high senescent status is associated with a decreased expression of the von Willebrand factor, suggesting a putative endothelial-to-mesenchymal transition (EndoMT) process. To go further, we analyzed the

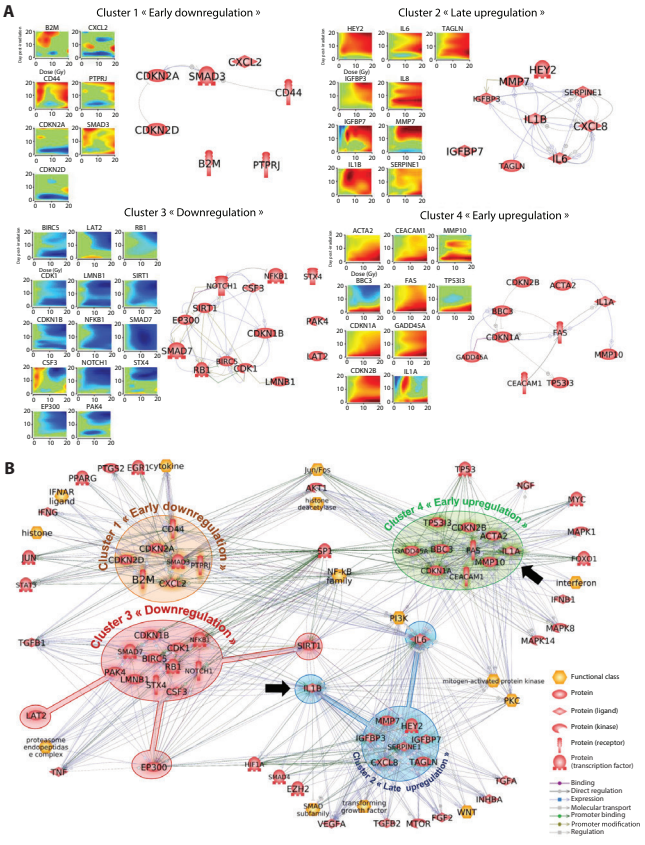


**Fig. 3.** Global network inference of the senescence-associated dynamic transcriptional program in human umbilical vein endothelial cells. (A) A similarity distance-based clustering method revealed 4 main clusters (1 to 4) of mRNA expression variation, and a network inference with a text mining-based tool was constructed for each cluster. (B) Global network inference of the senescence-associated dynamic transcriptional program in endothelial cells was inferred in order to identify putative key nodes.

expression of 2 endothelial markers (CD34 and von Willebrand factor), 2 mesenchymal markers (TAGLN and VIM), and the 2 main cytokines from the SASP. The results clearly showed that a high senescent status (IL8 and IL6 high) is associated with both a decreased expression of endothelial markers and an increased expression of mesenchymal markers (Fig. 5D).

## IL-1–dependent signaling pathway is involved in the radiation-induced EC SASP and radiation-induced senescence

Because the literature showed that a combination of IL-1A and TGFB2 is a powerful inductor of EndoMT in vitro by autocrine/paracrine activities,[26,27] we analyzed the expression of these markers at the single-cell level. The results of IL-1A, TGF-B2, and IL1R1 analyses strongly suggest a putative crucial role of the IL-1–dependent signaling pathway in the radiation-induced senescent phenotype of ECs (Fig. 6A). A subnetwork related to the IL-1 signaling pathway identifying all molecular relationships with a broad representation of deregulated genes observed in irradiated HUVECs was built and highlighted in blue (Fig. 6B). To validate the role of the IL-1 pathway in radiation-induced endothelial senescence, we silenced IL1R1 in ECs before irradiation and analyzed the effects on senescence (Fig. E15A). The IL1R1 knockdown led to approximately 20% fewer senescent cells 7 days after irradiation (Fig. 6C). mRNA level of IL1R1 return to a control level 7 days after irradiation (Fig E15B) explaining probably the statistically significant but relatively modest effect on senescence level. However, interistingly, TLDA experiments showed that IL1R1 silencing led to a reduced senescence-associated molecular profile, 3 and 7 days after irradiation (Figs. 6D and 6E).

## Discussion

We developed a step-by-step approach to provide rational evidence that HUVECs are an excellent in vitro model to study stress-induced senescence. To our knowledge, our results are the first based on an unbiased systematic comparison of EC types according to their response to radiation-induced senescence. We demonstrated that irradiated HUVECs recapitulate the overall endothelium

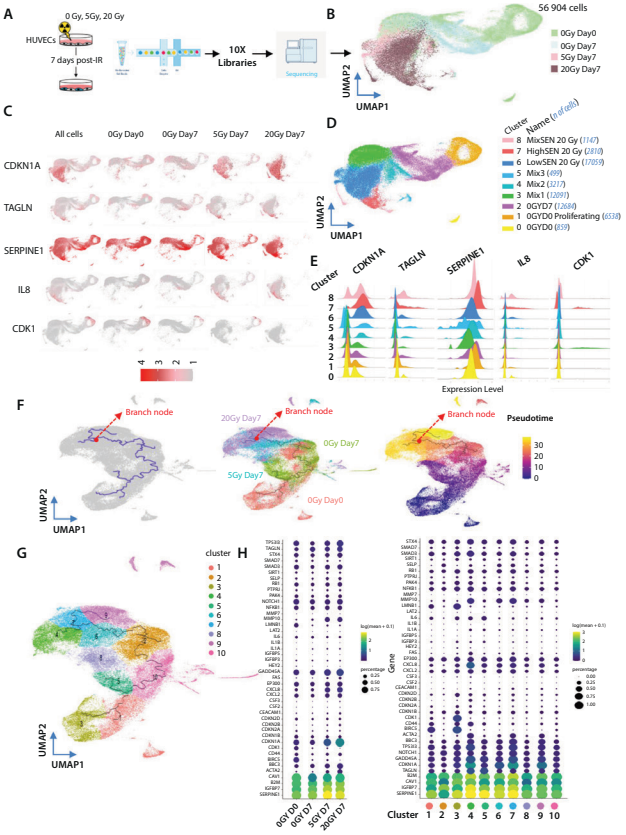


**Fig. 4.** Irradiation leads to a heterogeneous senescent status in endothelial cells, and pseudotime analysis reveals a crucial molecular transition node in irradiated cells that leads to a high senescent status. (A) Summary of scRNA-Seq workflow leads to a data matrix of 56,904 cells obtained from two biological replicates. (B) Global UMAP of 56,904 cells identified by irradiation doses. (C) UMAP visualizations of CDKN1A, TAGLN, SERPINE1, IL8, and CDK1 mRNA expression at the single-cell level are shown. (D) Cell clusterization showing the heterogeneous status of 20 Gy-exposed cells 7 days after irradiation. (E) Examples of ridgeline plots for CDKN1A, TAGLN, SERPINE1, IL8, and CDK1 mRNA expression in each cluster. (F) Pseudotime analysis showing the main path leading to a high senescent status. A crucial transition node is observed leading to a different senescent status in 20 Gy irradiated cells. UMAP visualization is shown according to all cells, to the group and to the pseudotime. (G) Unsupervised pseudotime clustering of all cells using the Louvain algorithm. (H) Dot plots representing the proportion of cells (circle size) and the mean expression (circle color) of the signature of the 44 genes associated with senescence. Dose-specific and cluster-specific results are shown. The results show that cluster 4 is characterized by a high senescent status with high levels of both CXCL8/IL8 and SERPINE1.

transcriptional program and strongly suggest that radiation-induced premature senescence in HUVECs can be used to explore senescence-associated endothelial dysfunctions in the pathological aging process. We deciphered the dynamic transcriptional program of radiation-induced EC senescence and showed noncell-autonomous effects, which strongly suggest that the endothelium can affect the senescent phenotype of other cell types by paracrine effects in vivo. Ritschka et al recently reported that transient exposure to a senescence-messaging secretome induces plasticity and provides regenerative signals, whereas prolonged exposure subsequently blocks growth-promoting signals, resulting in paracrine senescence responses and decreased regenerative capacity.[28] Moreover, radiation-induced EC senescence promotes a pro-atherosclerotic phenotype and monocyte adhesion by an epigenetic activation of CD44 expression, suggesting the ability of senescent ECs to control inflammation.[9]

Hernandez-Segura et al reported the importance of dynamic variations in fibroblasts and in the cell-specific heterogeneity of the senescence program.[21] Our in vitro results confirm that time series measurements provide crucial information and that biomathematical network-based clustering analyses reveal putative molecular hubs able to limit the progression of senescence. A panel of several molecular hubs has been extracted from our analysis, including the SIRT1, SP1, SMAD7, and IL-1 signaling pathways. Moreover, scRNA-Seq experiments revealed that radiation exposure induces a heterogeneous senescent status and that transcriptional heterogeneity is a hallmark of senescence. To our knowledge, only 1 work had addressed the heterogeneity of the senescent status of EC using such an approach.

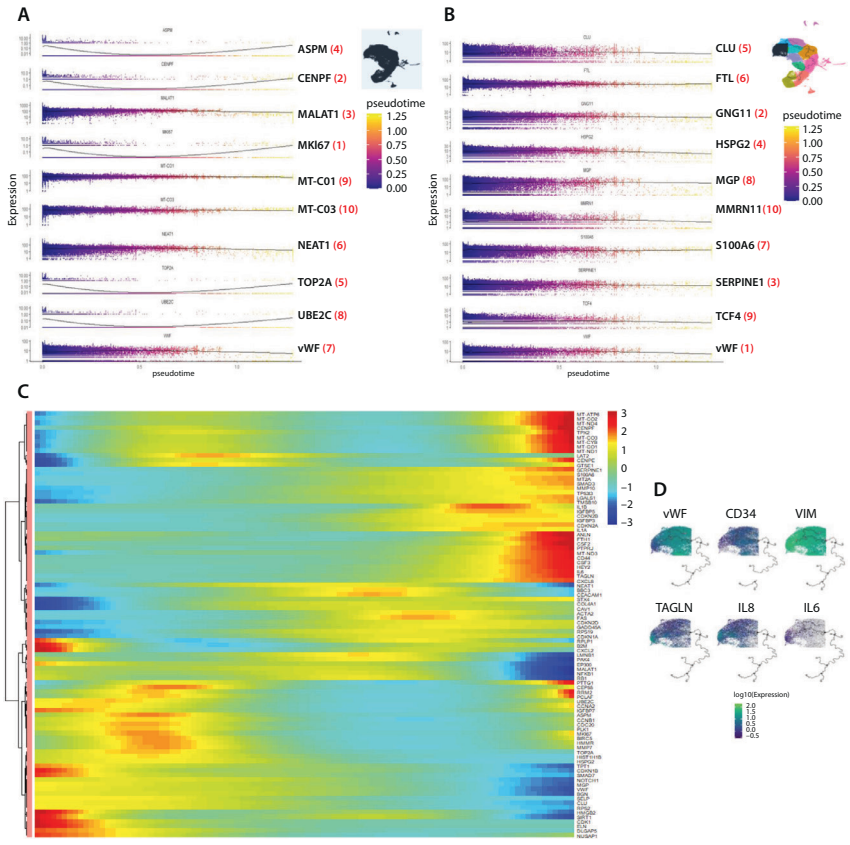


**Fig. 5.** A high senescent status is associated with an endothelial-to-mesenchymal transition phenotype. In-depth analysis using the Moran's I test function was performed to find genes that change in expression as a function of pseudotime. This method made it possible to find and classify genes that are differentially expressed across a single-cell trajectory, either on the entire trajectory or on only part of the trajectory focusing on some of the cells. The full lists and ranking of the top 300 genes are provided in Table E1, and were established based on either the entire trajectory; on the part to the left of the transition node, toward the high senescent status (ie, toward cluster 4); or the part to the right of the transition node, toward clusters 7 to 9. This was also established for the 44 genes of the signature (Fig. E14). (A) Expression of the top 10 genes along the main path of the pseudotime. The number in red between brackets indicates the rank. (B) Expression of the top 10 genes to the left of the transition node, toward the high senescent status. The number in red between brackets indicates the rank. (C) Aggregated heat map combining the signature of the 44 genes associated with senescence and the top 50 genes explaining the trajectory from the scRNA-Seq experiments. The results show changes for all genes through pseudotime as well as modules of genes that have similar expression patterns. (D) The mRNA level of 2 endothelial cell markers (vWF and CD34), 2 mesenchymal markers (TAGLN and VIM), and 2 senescence-associated secretory phenotype markers (IL6 and CXCL8/IL8), showing an endothelial-to-mesenchymal transition phenotype associated with markers of senescence.

Zirkel et al performed scRNA-Seq experiments to compare proliferating and arrested replicatively senescent HUVECs, showing that HMGB2 depletion within the nucleus is an early molecular event leading to chromatin remodeling and thus replicative senescence.[25] We also showed that HMGB2 loss is a marker of a radiation-induced senescent status (Fig. E12), supporting the results of Zirkel and colleagues and showing that HMGB2 depletion is shared by premature and replicative senescence. Moreover, scRNA-Seq results also showed that senescence is associated with both a decrease in endothelial marker expression and an increased mesenchymal marker expression. EndoMT is a process whereby an EC undergoes a series of molecular events that result in a mesenchymal cell phenotype involved in fibrotic disorders.[29,30] It was recently demonstrated that EndoMT is involved in radiation-induced normal tissue injury, such as radiation induced lung fibrosis[31] and proctitis,[22] and that conditional endothelial deletion reduces the frequency of EndoMT as well as the severity of radiation-induced normal tissue damage.[15] Radiation-induced EC senescence and the radiation-induced EndoMT phenotype share a large panel of characteristics suggesting that, in some circumstances, this could be the same phenomenon. Rieder and colleagues showed that human intestinal microvascular ECs undergo an EndoMT and contribute to fibrosis in human and experimental preclinical models of chronic inflammation.[27] They demonstrated in vitro that EndoMT is provoked by a

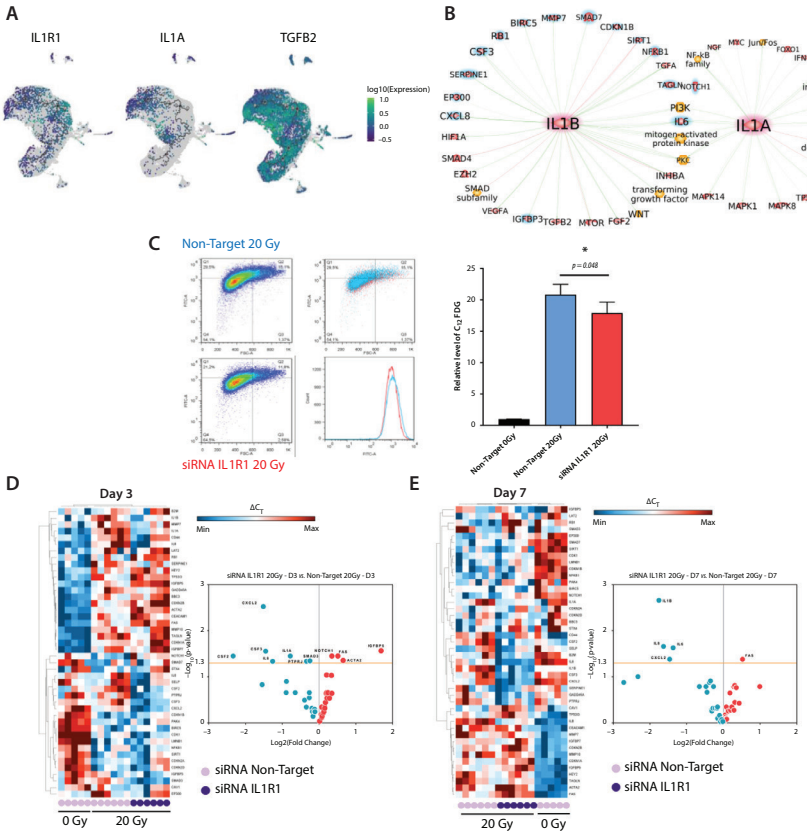


**Fig. 6.** The IL-1 signaling pathway affects radiation-induced senescence-associated secretory phenotype and senescence in endothelial cells in vitro. (A) The mRNA level of 3 key factors in the endothelial-to-mesenchymal transition phenotype, ie, IL1R1, IL-1A, and TGFB2, suggesting that 1, several, or all could be involved in the senescence-associated endothelial-to-mesenchymal transition phenotype. (B) Datamining-based network inference, showing a relationship between molecular entities and IL-1−dependent signaling as a hub to affect senescence. Entities with a blue halo were measured in these experiments. (C) Human umbilical vein endothelial cells (HUVECs) were transfected with IL1R1 siRNA in order to limit the IL-1−dependent signaling pathway. The senescence rates were monitored using $C_{12}$FDG cleavage detection. Results presented are from four independent biological replicates. Error bar = SD; significant difference assessed by unpaired *t* test, $P = .048$; *t* value = 2.47, DF = 6; n=4. (D) Heat map of TLDA analysis obtained at 3 days and (E) 7 days based on HUVECs and irradiated HUVECs transfected with IL1R1 siRNA. Volcano plots obtained at day 3 and day 7 based on irradiated HUVECs transfected with either non-targeting siRNA or IL1R1 siRNA are shown. Results presented are from 5 to 6 biological replicates.

combination of TGF-$\beta$1, IL-1$\beta$ and TNF-$\alpha$ with the powerful effect of IL-1.

In our work, we identified CD9 as a putative strong molecular player in radiation-induced EC senescence (Fig. E13). CD9, a cell surface glycoprotein belonging to the tetraspanin family, was recently shown as a regulator of replicative EC senescence through a PI3K-AKT-mTOR-p53-dependent pathway.[24] The silencing of CD9 in HUVECs as well as treatment with rapamycin, an mTOR inhibitor, reverse the senescent phenotype of ECs and reduce IL-1 and IL-6 production. Moreover, rapamycin was shown to inhibit EndoMT in HUVECs in vitro[32] and reverses the protein expression patterns of EndoMT in vivo,[33] arguing again that EndoMT could be a "senescent-like" phenotype. Rapamycin limits radiation-induced lung fibrosis after fractionated total thoracic irradiation in mice, reducing inflammatory cytokine expression and the level of senescent type II pneumocytes.[34]

Our results open a wide array of molecular strategies to try to limit radiation-induced senescence. In our work, we wanted to prove that targeting one molecular node could affect senescence and the SMS. The rationale for targeting the IL-1 signaling pathway was to find a putative molecular hub that controls EndoMT as well as a large panel of SASP-associated secretory proteins without affecting the molecular entities associated with cell cycle progression. Here, by targeting IL1R1, we demonstrated that the IL-1 signaling pathway affects the SASP of ECs as well as the degree of senescence, showing that IL-1 could be a good therapeutic target to limit senescence and non-cell-autonomous paracrine effects. IL-1$\alpha$ and IL-1$\beta$ KO mice exhibit a prolonged ovarian lifespan by reducing the expression of inflammatory

genes.[35] In vitro, inhibition of the IL-1 signaling pathway by different strategies reduced senescence-associated IL-6/IL-8 secretion in HCA2 primary foreskin fibroblasts.[36] Recently, in a mouse model of vascular radiation injury, Christersdottir et al showed that the IL-1 receptor antagonist Anakinra reduced arterial inflammation, suggesting that this inhibitor could be a treatment to prevent late radiation-induced vascular diseases.[37] The effect of eliminating senescent ECs in other physiopathological situations is currently being debated in the community, and this question must also be addressed in depth after radiation exposure as a cure for cancer.[38]

## Conclusions

Our work is a comprehensive study deciphering the dynamic of the radiation-induced senescence program, including both dose-effect and time parameters. The next step will be to understand the effect of the heterogeneous status on endothelial dysfunction in vivo, and more generally on normal tissue injury. Given the prolonged life expectancy of cancer survivors treated with RT alone or in combination with immunotherapy,[39] it will be important to better understand senescence-associated long term effects.

## References


1. Kuilman T, Peeper DS. Senescence-messaging secretome: SMS-ing cellular stress. *Nature Rev Cancer* 2009;9:81–94.
2. Herranz N, Gil J. Mechanisms and functions of cellular senescence. *J Clin* 2018;128:1238–1246.
3. Demaria M, Ohtani N, Youssef SA, et al. An essential role for senescent cells in optimal wound healing through secretion of PDGF-AA. *Dev Cell* 2014;31:722–733.
4. Ferreira-Gonzalez S, Lu WY, Raven A, et al. Paracrine cellular senescence exacerbates biliary injury and impairs regeneration. *Nat Comm* 2018;9:1020.
5. Prasanna PG, Citrin DE, Hildesheim J, et al. Therapy-induced senescence: Opportunities to improve anti-cancer therapy. *J Natl Cancer Inst* 2021 Oct 1;113(10):1285–1298.
6. Erusalimsky JD. Vascular endothelial senescence: From mechanisms to pathophysiology. *J Appl Physiol* 2009;106:326–332.
7. Wang Y, Boerma M, Zhou D. Ionizing radiation-induced endothelial cell senescence and cardiovascular diseases. *Radiat Res* 2016;186:153–161.
8. Lafargue A, Degorre C, Corre I, et al. Ionizing radiation induces long-term senescence in endothelial cells through mitochondrial respiratory complex II dysfunction and superoxide generation. *Free Radic Biol Med* 2017 Jul;108:750–759.
9. Lowe D, Raj K. Premature aging induced by radiation exhibits pro-atherosclerotic effects mediated by epigenetic activation of CD44 expression. *Aging Cell* 2014;13:900–910.
10. Soysouvanh F, Benadjaoud MA, Dos Santos M, et al. Stereotactic lung irradiation in mice promotes long-term senescence and lung injury. *Int J Radiat Oncol Biol Phys* 2020;106:1017–1027.
11. Pan J, Li D, Xu Y, et al. Inhibition of Bcl-2/xl with ABT-263 selectively kills senescent type ii pneumocytes and reverses persistent pulmonary fibrosis induced by ionizing radiation in mice. *Int J Radiat Oncol Biol Phys* 2017;99:353–361.
12. Abderrahmani R, Francois A, Buard V, et al. PAI-1-dependent endothelial cell death determines severity of radiation-induced intestinal injury. *PloS One* 2012;7:e35740.
13. Guipaud O, Jaillet C, Clément-Colmou K, François A, Supiot S, Milliat F. The importance of the vascular endothelial barrier in the immune-inflammatory response induced by radiotherapy. *Br J Radiol* 2018;91 20170762.
14. Paris F, Fuks Z, Kang A, et al. Endothelial apoptosis as the primary lesion initiating intestinal radiation damage in mice. *Science* 2001;293:293–297.
15. Mintet E, Lavigne J, Paget V, et al. Endothelial hey2 deletion reduces endothelial-to-mesenchymal transition and mitigates radiation proctitis in mice. *Sci Rep* 2017;7:4933.
16. Rannou E, Francois A, Toullec A, et al. In vivo evidence for an endothelium-dependent mechanism in radiation-induced normal tissue injury. *Sci Rep* 2015;5:15738.
17. Toullec A, Buard V, Rannou E, et al. HIF-1alpha deletion in the endothelium, but not in the epithelium, protects from radiation-induced enteritis. *Cell Mol Gastroenterol Hepatol* 2018;5:15–30.
18. Abderrahmani R, Francois A, Buard V, et al. Effects of pharmacological inhibition and .genetic deficiency of plasminogen activator inhibitor-1 in radiation-induced intestinal injury. *Int J Radiat Oncol Biol Phys* 2009;74:942–948.
19. Milliat F, Sabourin JC, Tarlet G, et al. Essential role of plasminogen activator inhibitor type-1 in radiation enteropathy. *Am J Pathol* 2008;172:691–701.
20. Soto-Gamez A, Quax WJ, Demaria M. Regulation of survival networks in senescent cells: From mechanisms to interventions. *J Mol Biol* 2019;431:2629–2643.
21. Hernandez-Segura A, de Jong TV, Melov S, Guryev V, Campisi J, Demaria M. Unmasking transcriptional heterogeneity in senescent cells. *Curr Biol* 2017;27:2652–2660.
22. Mintet E, Rannou E, Buard V, et al. Identification of endothelial-to-mesenchymal transition as a potential participant in radiation proctitis. *Am J Pathol* 2015;185:2550–2562.
23. Debacq-Chainiaux F, Erusalimsky JD, Campisi J, Toussaint O. Protocols to detect senescence-associated beta-galactosidase (SA-betagal) activity, a biomarker of senescent cells in culture and in vivo. *Nat Protoc* 2009;4:1798–1806.
24. Cho JH, Kim EC, Son Y, et al. CD9 induces cellular senescence and aggravates atherosclerotic plaque formation. *Cell Death Differ* 2020;27:2681–2696.
25. Zirkel A, Nikolic M, Sofiadis K, et al. HMGB2 loss upon senescence entry disrupts genomic organization and induces CTCF clustering across cell types. *Mol Cell* 2018;70:730–744 e6.
26. Medici D, Potenta S, Kalluri R. Transforming growth factor-beta2 promotes snail-mediated endothelial-mesenchymal transition through convergence of Smad-dependent and Smad-independent signalling. *Biochem J* 2011;437:515–520.
27. Rieder F, Kessler SP, West GA, et al. Inflammation-induced endothelial-to-mesenchymal transition: A novel mechanism of intestinal fibrosis. *Am J Pathol* 2011;179:2660–2673.
28. Ritschka B, Storer M, Mas A, et al. The senescence-associated secretory phenotype induces cellular plasticity and tissue regeneration. *Genes Dev* 2017;31:172–183.
29. Zeisberg EM, Tarnavski O, Zeisberg M, et al. Endothelial-to-mesenchymal transition contributes to cardiac fibrosis. *Nat Med* 2007;13:952–961.
30. Zhang Y, Wu X, Li Y, et al. Endothelial to mesenchymal transition contributes to arsenic-trioxide-induced cardiac fibrosis. *Sci Rep* 2016;6: 33787.
31. Lavigne J, Suissa A, Verger N, et al. Lung stereotactic arc therapy in mice: Development of radiation pneumopathy and influence of hif-1alpha endothelial deletion. *Int J Radiat Oncol Biol Phys* 2019;104:279–290.
32. Tian D, Zeng X, Wang W, Wang Z, Zhang Y, Wang Y. Protective effect of rapamycin on endothelial-to-mesenchymal transition in HUVECs through the Notch signaling pathway. *Vascul Pharmacol* 2019;113:20–26.

33. Ranchoux B, Antigny F, Rucker-Martin C, et al. Endothelial-to-mesenchymal transition in pulmonary hypertension. *Circulation* 2015;131:1006–1018.
34. Chung EJ, Sowers A, Thetford A, et al. Mammalian target of rapamycin inhibition with rapamycin mitigates radiation-induced pulmonary fibrosis in a murine model. *Int J Radiat Oncol Biolo Phys* 2016;96:857–866.
35. Uri-Belapolsky S, Shaish A, Eliyahu E, et al. Interleukin-1 deficiency prolongs ovarian lifespan in mice. *Proc Natl Acad Sci U S A* 2014;111:12492–12497.
36. Orjalo AV, Bhaumik D, Gengler BK, Scott GK, Campisi J. Cell surface-bound IL-1alpha is an upstream regulator of the senescence-associated IL-6/IL-8 cytokine network. *Proc Natl Acad Sci U S A* 2009;106:17031–17036.
37. Christersdottir T, Pirault J, Gistera A, et al. Prevention of radiotherapy-induced arterial inflammation by interleukin-1 blockade. *Eur Heart J* 2019;40:2495–2503.
38. Martin N, Huna A, Bernard D. Elimination of senescent endothelial cells: Good or bad idea? *Trends Cell Biol* 2021;31:327–330.
39. Mondini M, Levy A, Meziani L, Milliat F, Deutsch E. Radiotherapy-immunotherapy combinations—perspectives and challenges. *Mol Oncol* 2020;14:1529–1537.